Doublon-Holon Origin of the Subpeaks at the Hubbard Band Edges

Seung-Sup B. Lee, Jan von Delft, and Andreas Weichselbaum
Physics Department, Arnold Sommerfeld Center for Theoretical Physics and Center for NanoScience, Ludwig-Maximilians-Universität München, Theresienstraße 37, 80333 München, Germany
(Received 10 May 2017; published 5 December 2017)

Dynamical mean-field theory (DMFT) studies frequently observe a fine structure in the local spectral function of the SU(2) Fermi-Hubbard model at half filling: In the metallic phase close to the Mott transition, subpeaks emerge at the inner edges of the Hubbard bands. Here we demonstrate that these subpeaks originate from the low-energy effective interaction of doublon-holon pairs, by investigating how the correlation functions of doublon and holon operators contribute to the subpeaks. A mean-field analysis of the low-energy effective Hamiltonian provides results consistent with our DMFT calculation using the numerical renormalization group as an impurity solver. In the SU(3) and SU(4) Hubbard models, the subpeaks become more pronounced due to the increased degeneracy of doublon-holon pair excitations.

DOI: 10.1103/PhysRevLett.119.236402

Introduction.—The dynamical mean-field theory (DMFT) [1] provides a widely successful approach in understanding strongly correlated systems. It treats a lattice problem by self-consistently solving an effective impurity model whose impurity and bath correspond to a lattice site and the rest of the lattice, respectively. Thus, the performance of DMFT calculations directly depends on which particular impurity solver is chosen.

A benchmark calculation for various impurity solvers is the paramagnetic Mott transition in the half-filled SU(2) Hubbard model at temperature $T = 0$ which is characterized by a striking change in the local spectral functions [2,3]. In the metallic phase, the spectral function features a quasiparticle peak (QP) at the Fermi level and two Hubbard bands (HBs) below and above the Fermi level each. In the insulating phase, the QP disappears and a gap opens between two HBs.

In the metallic phase close to the transition, many DMFT studies have observed sharp subpeaks that emerge at the inner edges of the HBs, by using different real-frequency impurity solvers: perturbative methods [2], the density-matrix renormalization group (DMRG) [4–7], the numerical renormalization group (NRG) [8], and exact diagonalization [9,10]. In contrast, quantum Monte Carlo solvers, which obtain the spectral functions on the real frequency axis via (numerically ill-posed) analytic continuation, have not found these subpeaks. The subpeaks give rise to distinct features in the momentum-resolved spectral function [5], measurable by photoemission spectroscopy [11,12]. Despite these frequent consistent observations, the physical origin of the subpeaks and their relevance in more general (e.g., multiflavor) models remained unclear.

In this Letter, we show that the subpeaks are induced by the effective doublon-holon (DH) [13] pair interaction originating from a second-order virtual process, where a doublon (holon) means an excitation that one particle is added to (removed from) a lattice site with average integer filling. We compute the correlation functions of doublon and holon operators in the SU(2) Hubbard model, by using the DMFT with NRG [14,15] as an impurity solver, and demonstrate that these correlation functions manifest the peak structure associated with the subpeaks. We reproduce the peak structure of doublon and holon correlators via a mean-field analysis of the low-energy effective Hamiltonian obtained by a generalized Schrieffer-Wolff transformation (SWT) [16,17]. Both approaches consistently result in a linear dependence of the subpeak position vs interaction strength. From our DMFT + NRG calculations of general SU(N) Hubbard models for $N = 2$, 3, 4, we observe that the subpeaks become more pronounced with increasing N, since the DH pair excitations become more degenerate due to the larger SU(N) symmetry.

System.—The SU(N) Hubbard model describes N flavors of fermions on a lattice with local repulsive interactions, recently realized in ultracold atom experiments with tunable N [18]. The hopping amplitude v, the interaction strength U, and the chemical potential are flavor independent; thus, the system has SU(N) flavor symmetry. Its Hamiltonian is $H = H_U + H_v + H_\mu$, where $H_U = (U/2)\sum_i (\hat{n}_i - \bar{n})^2$, $H_v = v\sum_{\langle i,j\rangle,\nu} c^\dagger_{i\nu} c_{j\nu}$ + H.c., and $H_\mu = -\mu\sum_i \hat{n}_i$. Here $c_{i\nu}$ annihilates a particle of flavor $\nu = 1, \ldots, N$ at lattice site i, $\hat{n}_i = \sum_\nu c^\dagger_{i\nu} c_{i\nu}$ is the particle number operator at site i, $\langle i, j\rangle$ indicates nearest neighbors, $\bar{n}$ is a parameter for the desired average occupation, and μ is a fine-tuning of the chemical potential to achieve $\langle \hat{n}_i \rangle = \bar{n}$. Throughout this Letter, we focus on $T = 0$ and the average occupation number as an integer closest to half filling $\bar{n} = \lfloor N/2 \rfloor$, by fixing $\mu = 0$ for $N = 2, 4$ and fine-tuning μ for $N = 3$.

Doublon and holon.—For integer average occupation $\bar{n}$, we define the doublon and holon creation operators as

$$d^\dagger_{i\nu} \equiv P_{i,\bar{n}+1} c^\dagger_{i\nu}, \qquad h^\dagger_{i\nu} \equiv P_{i,\bar{n}-1} c_{i\nu}, \tag{1}$$

where P_{in} means the projector onto the subspace in which the site i has n particles. For the SU(2) case, at half filling, $\bar{n} = 1$, these operators reduce to $d_{i\nu} = c_{i\nu}\hat{n}_{i\bar{\nu}}$ and $h_{i\nu} = c^\dagger_{i\nu}(1 - \hat{n}_{i\bar{\nu}})$ with $\hat{n}_{i\nu} = c^\dagger_{i\nu} c_{i\nu}$ and $\bar{\nu} = 3 - \nu$, and they completely constitute the particle operator $c_{i\nu} = d_{i\nu} + h^\dagger_{i\nu}$. Then the particle correlator can be decomposed into four doublon and holon correlators: $A_{cc^\dagger}(\omega) = A_{dd^\dagger} + A_{dh} + A_{h^\dagger d^\dagger} + A_{h^\dagger h}$, where $A_{XY}(\omega) \equiv (-1/\pi)\mathrm{Im}G_{XY}$, with $G_{XY}(t) = -i\vartheta(t)\langle[X(t), Y(0)]_\pm\rangle_T$ being the retarded correlation function of the fermionic (+) or bosonic (−) local operators X and Y acting on the same site. In the particle-hole symmetric case, only two correlators are independent: "diagonal" correlators $A_{dd^\dagger}(\omega) = A_{h^\dagger h}(-\omega)$, which are asymmetric, and "off-diagonal" correlators $A_{h^\dagger d^\dagger}(\omega) = A_{dh}(\omega)$, which are symmetric under $\omega \leftrightarrow -\omega$. For $N > 2$ flavors, the decomposition of $c_{i\nu}$ acquires more terms than $d_{i\nu}$ and $h^\dagger_{i\nu}$ [17].

DMFT+NRG.—We use the single-site DMFT, which maps the Hubbard model onto the single-impurity Anderson model (SIAM) which provides paramagnetic solutions, by construction. We employ the semicircular density of states of the Bethe lattice with half-bandwidth D, together with units $D = \hbar = k_B = 1$, throughout. We solve the SIAM by the full-density-matrix NRG (fdm-NRG; [19]), exploiting $\mathrm{U}(1)_{\mathrm{charge}} \otimes \mathrm{SU}(N)_{\mathrm{flavor}}$ symmetry [20]. The coarse-grained discretization-averaged spectral data are broadened adaptively [21,25] for the best possible spectral resolution at higher energies while preserving the intrinsic accuracy of the NRG at low energies [e.g., the Luttinger pinning [26] $(\pi/2)A(\omega = 0) = 1$ in the metallic phase is accurately satisfied; see Figs. 1(a) and 1(b)].

SU(2) *metallic phase.*—We first consider the case $N = 2$ equivalent to the spin-full one-band Hubbard model. At $T = 0$ and half filling, a metallic phase exists for $U < U_{c2} = 2.91(1)$ and a paramagnetic insulating phase for $U > U_{c1} = 2.37(2)$. For $U_{c1} < U < U_{c2}$, the two phases coexist (e.g., see Fig. 2 or Refs. [3,27]).

Within the metallic phase, the local spectral function $A(\omega)$ features one QP and two HBs [cf. Figs. 1(a) and 1(b)]. As U increases, the central QP narrows, the HBs widen, and the dips between the QP and the HBs deepen. On top of this, subpeaks are present at the inner edges of the HBs, whose position ω_p and width $\delta\omega$ decrease linearly with increasing U, as shown in Fig. 2.

Local spin (i.e., flavor) and charge susceptibilities χ_s and χ_c [28], respectively, in Fig. 1 demonstrate that the QP and the HBs of $A(\omega)$ are tied to spin and charge degrees of freedom, respectively; that is, spin and charge excitations are energetically separated. The peak of χ_s indicates a spinlike collective mode responsible for the QP, which is analogous to the Kondo resonance in the SIAM in that the spin susceptibility peaks at the Kondo energy scale [29]. The position ω_s and width of the χ_s peak decrease as the QP narrows with increasing U; especially, ω_s has a linear

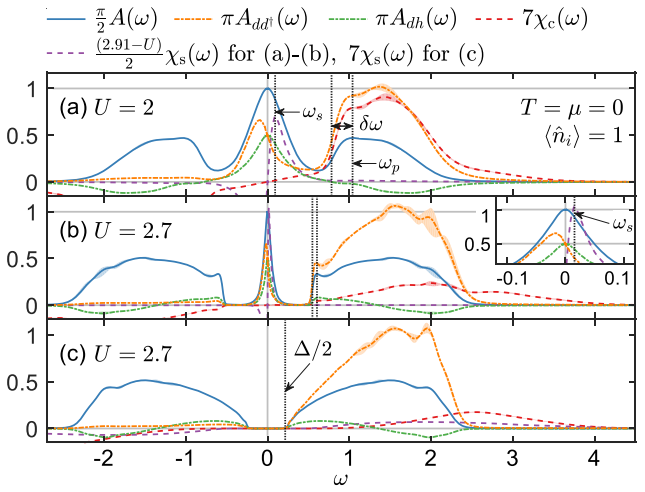

FIG. 1. Local correlation functions in (a),(b) the metallic and (c) insulating phases of the SU(2) Hubbard model: the local spectral function $A(\omega)$ (blue solid lines), the correlators of doublon $d_{i\nu}$ and holon $h_{i\nu}$ operators [cf. Eq. (1)] (dash-dotted lines), charge susceptibility $\chi_c = A_{\delta\hat{n},\delta\hat{n}}$ (red dashed lines), and spin (i.e., flavor) susceptibility $\chi_s = A_{\vec{S},\vec{S}}/3$ (purple dashed lines), with $\chi_{c(s)}(\omega) = -\chi_{c(s)}(-\omega)$, $A_{dd^\dagger}(\omega) = A_{h^\dagger h}(-\omega)$, and $A_{dh}(\omega) = A_{h^\dagger d^\dagger}(\omega)$. Here $\delta\hat{n}_i \equiv \hat{n}_i - \langle\hat{n}_i\rangle$, and $\vec{S}_i$ is the spin operator at site i. Each correlator is averaged over different discretizations (see Sec. I B of Ref. [21]), where the corresponding color-matched shaded area provides an estimate for numerical uncertainties, noticeable only in the HBs. Panels (b) and (c) show different solutions for the same value of U in the coexistence regime. In (b), the inset enlarges the region of the QP. We mark the location of spectral features by vertical dotted lines: (a),(b) subpeak position ω_p (defined as the local maximum near the inner HB edge), subpeak width $\delta\omega$ [defined as the minimum positive value satisfying $A(\omega_p - \delta\omega) = A(\omega_p)/2$], spin susceptibility peak position ω_s, and (c) inner HB edge at $\Delta/2$, where Δ is the Mott gap.

dependence vs $1/U$, as shown in Fig. 2. In contrast, χ_c is suppressed within the QP region while having long tails beyond the outer edges of the HBs.

For $T = 0^+$, the positive and negative energy sides of a correlator $A_{XY}(\omega)$ are derived from $\langle X(t)Y(0)\rangle_T$ and

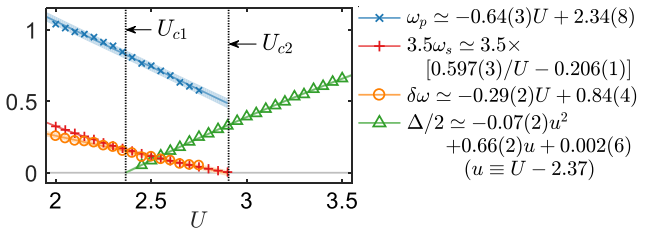

FIG. 2. The U dependence of the spectral features: the position ω_p and width $\delta\omega$ of the subpeaks, the peak position ω_s of spin susceptibility χ_s, and the Mott gap Δ (cf. Fig. 1). Symbols are data points from the DMFT + NRG calculations, lines are fits, and shading gives the 95% prediction bounds of fitting. The zeros of the extrapolated fits of Δ and ω_s yield estimates for the critical interaction strengths $U_{c1} = 2.37(2)$ and $U_{c2} = 2.91(1)$, respectively.

$\langle Y(0)X(t)\rangle_T = \langle X^\dagger(t)Y^\dagger(0)\rangle_T^*$, respectively. Therefore, the upper HB in Fig. 1, which mainly consists of $A_{dd^\dagger}$, originates from the dynamics of the doublon $d_{i\nu}^\dagger(0)$. Another significant feature of $A_{dd^\dagger}$ is a peak at $\omega = -\omega_s$. Just after the action of $d_{i\nu}(0)$ and just before $d_{i\nu}^\dagger(t)$, the site i has only spin $\bar{\nu}$. Its time evolution between 0 and t with low frequency $|\omega| \simeq \omega_s$ is driven by the spinlike collective mode captured by the peak of χ_s at ω_s. In contrast, the off-diagonal correlator A_{dh} has a symmetric peak at $\omega = 0$. This reflects the particle-hole symmetric processes of destroying at the same site first a doublon and then a holon, or vice versa. $A_{dd^\dagger}$ and A_{dh} contribute comparably to the QP, having $A_{dd^\dagger}(0) = A_{dh}(0) = (1/2\pi)$.

In the metallic regime in Figs. 1(a) and 1(b), all of the doublon and holon correlators show peaklike features at $\omega = \pm\omega_p$. For $U \gtrsim 2.3$ [21], their contributions to these subpeaks have relative weights $A_{dd^\dagger}(\omega_p) > A_{dh}(\pm\omega_p) > A_{dd^\dagger}(-\omega_p)$. Our effective theory (described below) aims to reproduce this relative order of contributions as well as the linear dependence of ω_p vs U.

SU(2) *insulating phase.*—The QP, the subpeaks, the spin-charge separation in energy space, and the peaks of the doublon and holon correlators all disappear in the insulating phase, as depicted in Fig. 1(c). Instead, a Mott gap Δ opens, and the susceptibilities χ_s and χ_c spread over a large energy range $|\omega| > \Delta/2$ with suppressed heights. While both ω_p in the metallic phase and $\Delta/2$ in the insulating phase correlate to the location of the inner HB edges, their dependences on U are clearly different (see Fig. 2). Here the absence of subpeaks is consistent with previous studies [4–10]. Though other works [30–32] have reported subpeaks even in the insulating phase, their observations are not numerically stable due to, e.g., ill-posed analytic continuation or underbroadening.

DH pair interaction.—We will now demonstrate that the peaks of the doublon and holon correlators at $\omega = \pm\omega_p$, which add up to the subpeaks of $A(\omega)$, originate from a DH pair interaction within the low-energy effective Hamiltonian of the SU(2) Hubbard model. Our theory is based on the separation of three energy scales: $\omega_s < \omega_p < U/2$, corresponding to the QP, the subpeaks, and the HBs, respectively. We focus on the intermediate scale ω_p by integrating out the larger scale $U/2$ and by approximating the physics of the smaller scale ω_s.

We first integrate out the charge fluctuation of energy scale $U/2$, by employing a generalized SWT [16,17]. We decompose the hopping term into different components $H_v = \sum_{m=-1}^{+1} H_{v;m}$, which cost Coulomb energy mU since $mUH_{v;m} = [H_U, H_{v;m}]$. Here $H_{v;0} \equiv v\sum_{\langle i,j\rangle,\nu}(d_{i\nu}^\dagger d_{j\nu} - h_{i\nu}^\dagger h_{j\nu}) + \text{H.c.}$ describes the hopping of doublons and holons without an energy cost, whereas $H_{v;1} \equiv v\sum_{\langle i,j\rangle,\nu}(d_{i\nu}^\dagger h_{j\nu}^\dagger + d_{j\nu}^\dagger h_{i\nu}^\dagger)$ or $(H_{v;-1} = H_{v;1}^\dagger)$ creates (annihilates) nearest-neighbor DH pairs by paying (gaining) energy cost U. Then we write the low-energy effective Hamiltonian H_{eff} as a power series in v/U:

$$H_{\text{eff}} = H_{v;0} + H_{ss} + H_{dh} + H_{3\text{-site}} + O(v^3/U^2), \tag{2}$$

$$H_{ss} = \frac{v^2}{U}\sum_{\langle i,j\rangle} 4\vec{S}_i \cdot \vec{S}_j - P_{i1}P_{j1},$$

$$H_{dh} = \frac{2v^2}{U}\sum_{\langle i,j\rangle}(c_{j1}^\dagger c_{j2}^\dagger c_{i2}c_{i1} + P_{i2}P_{j0}) + (i \leftrightarrow j)$$

$$= \frac{v^2}{U}\sum_{\langle i,j\rangle,\nu,\nu'}(h_{i\nu}^\dagger d_{j\nu}^\dagger + h_{j\nu}^\dagger d_{i\nu}^\dagger)(d_{i\nu'}h_{j\nu'} + d_{j\nu'}h_{i\nu'}),$$

where $H_{3\text{-site}}$ is the sum of the products of operators at three nearest-neighbor sites. The term $H_{ss} + H_{dh} + H_{3\text{-site}} = [H_{v;1}, H_{v;-1}]/U$, of the order of $O(v^2/U)$, can be interpreted as second-order virtual processes. H_{eff} is similar to the *t-J* model [33], widely used as the effective low-energy model for a Mott insulator, but additionally contains a three-site term $H_{3\text{-site}}$ and, importantly, the DH term H_{dh}. Each term in Eq. (2) respects the $\text{SU}(2)_{\text{charge}} \otimes \text{SU}(2)_{\text{spin}}$ symmetry of the system. See Ref. [17] for a detailed derivation for general N. Hereafter we discard the higher-order $O(v^3/U^2)$ terms.

The low-energy Hamiltonian H_{eff} in Eq. (2) describes two effective nearest-neighbor interactions whose role and relevance depend on the phase of the system. (i) H_{ss} contains the Heisenberg spin-spin interaction. In our paramagnetic metallic phase, this interaction induces a spinlike collective mode of energy scale ω_s. The interaction strength v^2/U is consistent with the scaling of $\omega_s \sim 1/U$ (cf. Fig. 2). On the other hand, H_{ss} becomes irrelevant in the paramagnetic insulating phase, where the spin susceptibility χ_s is overall suppressed. (ii) H_{dh} describes a DH pair interaction which acts on the subspace with a finite number of DH pairs. Thus H_{dh} is relevant (irrelevant) in the metallic (insulating) phase.

Doublon and holon peaks.—After integrating out the largest energy scale U, we consider the doublon and holon dynamics governed by the effective Hamiltonian H_{eff}, aiming at the intermediate energy scale $\omega_p > \omega_s$, in the *metallic* phase. We simplify the physics at lower energies ($\lesssim\omega_s$) without exactly solving H_{eff}, by introducing two approximations described in detail in Ref. [17]. (i) We introduce a mean field, $\Delta_{dh} \equiv (v/2)\sum_\nu\langle d_{i\nu}h_{j\nu} + d_{j\nu}h_{i\nu}\rangle$, which regards the Fermi-liquid ground state as the "condensate" of the DH pairs. Then we approximate the DH interaction term as $H_{dh} \approx (v/U)\sum_{\langle i,j\rangle,\nu}\Delta_{dh}^*(d_{i\nu}h_{j\nu} + d_{j\nu}h_{i\nu}) + (\text{H.c.})$. The mean-field variable Δ_{dh}, comprised of the expectation value of the pair annihilation operator $d_{i\nu}h_{j\nu} + d_{j\nu}h_{i\nu}$, is reminiscent of the Bardeen-Cooper-Schrieffer theory. Here the situation is quite different, though, in that charge conservation is actually not broken, given that the pair annihilation operator is nothing but a summand of the decomposed hopping term $H_{v;-1}$. The DH pairs are singlets of the $\text{SU}(2)_{\text{charge}} \otimes \text{SU}(2)_{\text{spin}}$ symmetry preserved in the metallic phase, and the mean-field approximation of H_{dh} also respects that symmetry [17]. (ii) We decouple the doublon and holon correlators from

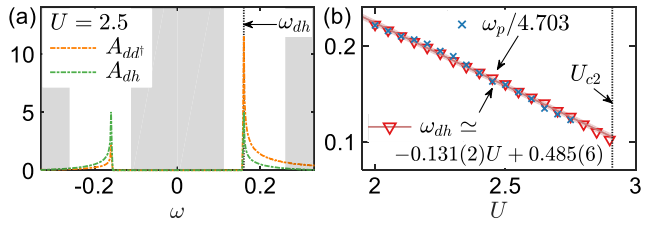

FIG. 3. (a) Doublon and holon correlators $A_{dd^\dagger}$ (orange dash-dotted line) and A_{dh} (green dash-dotted line) from our effective theory for the metallic phase. Lower-energy spin dynamics at energies $|\omega| \lesssim \omega_s$ and higher-energy scales $|\omega| \gtrsim U/2$ are neglected (as schematically indicated by the gray shading) by employing the generalized SWT together with a mean-field decoupling scheme. A_{dh} is symmetric, while $A_{dd^\dagger}$ is asymmetric. Both lines have a pair of peaks at $\omega = \pm\omega_{dh}$, showing $A_{dd^\dagger}(\omega_{dh}) > A_{dh}(\pm\omega_{dh}) > A_{dd^\dagger}(-\omega_{dh})$. This is qualitatively consistent with the DMFT + NRG results for $A_{dd^\dagger}$ and A_{dh} at $\omega = \pm\omega_p$ in Fig. 1(b) using the same color coding. (b) The peak position ω_{dh} from the effective theory decreases linearly with increasing U. The narrow shading gives the 95% prediction bounds of a linear fit. ω_{dh} nicely overlaps with ω_p (data taken from Fig. 2) up to an overall scaling factor. We take $\Delta_{dh} = 2.91 = U_{c2}$ independent of U, while the half-filled fraction $\langle P_{i1}\rangle$ is U dependent, with the data taken from our DMFT + NRG results [21].

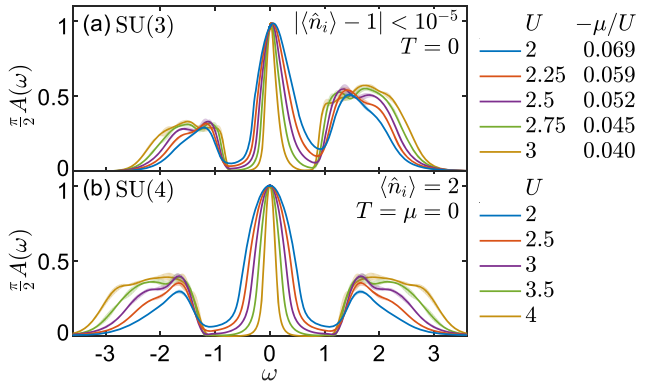

FIG. 4. Local spectral function $A(\omega)$ for (a) the SU(3) and (b) SU(4) Hubbard models in their metallic phases. Shading again reflects the uncertainties based on discretization averaging (cf. Fig. 1). For $N = 3$, the chemical potential μ was fine-tuned to have the integer filling $\langle\hat{n}_i\rangle \simeq 1$ for different U, as shown in the legend of (a). For $N = 4$, we have $\mu = 0$ due to particle-hole symmetry. In all cases, being in the metallic regime, subpeaks emerge at the inner HB edges.

charge and spin density fluctuations. This is based on the numerical results that they are characterized by different energy scales: Charge fluctuations are suppressed in the regime $|\omega| \lesssim U/2$, and spin fluctuations predominantly occur at energies $|\omega| \lesssim \omega_s$ (see Fig. 1). As a result, the equations of motion for the correlators close.

Figure 3(a) shows the resulting doublon and holon correlators for finite Δ_{dh} in the metallic phase. They have a pair of peaks at $\omega = \pm\omega_{dh}$, akin to their peaks at $\omega = \pm\omega_p$ in Fig. 1. Figure 3(b) demonstrates that the DH peak position ω_{dh} from the effective theory and the DMFT + NRG result of the subpeak position ω_p agree well up to an overall scaling factor of $\simeq$4.7, which may be expected to arise given the crudeness of our approximations. In contrast, in the insulating phase H_{dh} is irrelevant, such that $\Delta_{dh} = 0$. As a consequence, the subpeaks are absent in the insulating phase.

Predictions for photoemission spectroscopy.—The QP and the HBs of the local spectral functions have already been observed in photoemission spectroscopy [11,12]. This technique, which probes the momentum-resolved spectral function $A(\omega, \mathbf{k})$ [whose momentum average yields the local $A(\omega)$ discussed hitherto], should also be able to reveal the DH subpeaks. We have thus computed $A(\omega, \mathbf{k})$; see Figs. S3 and S4 of Ref. [21]. Our $T = 0$ results agree with prior DMFT + DMRG results from Ref. [5], showing that the feature in $A(\omega, \mathbf{k})$, which leads to the subpeak in $A(\omega)$, has distinct dispersion, consistent with the interpretation of DH pair propagation. Going beyond Ref. [5], we also analyze finite T and find that the subpeak-related features survive below the critical temperature for the Mott transition [21]. The distinct dispersion and T dependence of the subpeak, correlated with those of the QP, distinguish it from other fine structure of the HBs originating from atomic levels. We suggest to search for such features in photoemission data, especially in multiband materials where the subpeaks become more pronounced, as we discuss below.

SU($N > 2$) *models.*—We also analyze the SU(3) and SU(4) Hubbard models at integer filling $\langle\hat{n}_i\rangle = \lfloor N/2 \rfloor$, with the results shown in Fig. 4. Similar to the case $N = 2$ in Fig. 1, we again observe subpeaks on the inner edges of the HBs. While the subpeaks carry small weights compared with the rest of the HBs for $N = 2$ [cf. Fig. 1(b)], the subpeaks for $N = 3$, 4 have significantly larger relative weights (cf. purple lines in Fig. 4). Even for $N = 4$, the subpeaks are clearly higher than the rest of the HBs. Note that the QP persists more strongly at large $U \gtrsim 3$ for larger N, similarly to the widening of the Kondo peak in the SU(N) Kondo model [34].

We interpret this enhancement of the subpeaks as resulting from the enlarged space of DH pair excitations in the SU($N > 2$) Hubbard models. Generalizing the DH interaction H_{dh} discussed above to the SU($N > 2$) cases, we find that the DH pair excitations on nearest neighbors are threefold and 15-fold degenerate in the SU(3) and SU(4) models, respectively, in contrast to the nondegeneracy in the SU(2) case [17]. A particularly promising area for studying this behavior is ultracold atom physics, where pronounced DH correlations have been reported in the 2D Hubbard model [35].

Conclusion.—We showed that the subpeaks at the inner HB edges can be related to the effective DH pair interaction by using a generalized SWT. By using the NRG as a real-frequency impurity solver for the DMFT, we uncovered detailed dynamical information on the decomposition of the local spectral function into doublon and holon correlators. By utilizing a recently developed broadening scheme [25], we efficiently resolved those spectral features at high energies

which had been considered challenging for the NRG in the past due to its logarithmic coarse graining. An effective theory based on the scale separation of the characteristic energy scales ω_s, ω_p, and U reproduces the linear U dependence of ω_p found numerically in DMFT + NRG. Our predictions should be testable using photoemission spectroscopy of correlated materials or in ultracold atom systems.

We thank M. Bukov, G. Kotliar, A. Mitchell, K. Penc, A. Polkovnikov, M. Punk, and R. Žitko for fruitful discussion. This work was supported by Nanosystems Initiative Munich. S.-S. B. L. acknowledges support from the Alexander von Humboldt Foundation and the Carl Friedrich von Siemens Foundation and A. W. from the German Research Foundation (DFG) WE4819/2-1.

[1] A. Georges, G. Kotliar, W. Krauth, and M. J. Rozenberg, Rev. Mod. Phys. **68**, 13 (1996); G. Kotliar, S. Y. Savrasov, K. Haule, V. S. Oudovenko, O. Parcollet, and C. A. Marianetti, Rev. Mod. Phys. **78**, 865 (2006).
[2] X. Y. Zhang, M. J. Rozenberg, and G. Kotliar, Phys. Rev. Lett. **70**, 1666 (1993).
[3] R. Bulla, Phys. Rev. Lett. **83**, 136 (1999).
[4] M. Karski, C. Raas, and G. S. Uhrig, Phys. Rev. B **72**, 113110 (2005).
[5] M. Karski, C. Raas, and G. S. Uhrig, Phys. Rev. B **77**, 075116 (2008).
[6] M. Ganahl, P. Thunström, F. Verstraete, K. Held, and H. G. Evertz, Phys. Rev. B **90**, 045144 (2014); M. Ganahl, M. Aichhorn, H. G. Evertz, P. Thunström, K. Held, and F. Verstraete, Phys. Rev. B **92**, 155132 (2015).
[7] F. A. Wolf, I. P. McCulloch, O. Parcollet, and U. Schollwöck, Phys. Rev. B **90**, 115124 (2014).
[8] R. Žitko and T. Pruschke, Phys. Rev. B **79**, 085106 (2009).
[9] M. Granath and H. U. R. Strand, Phys. Rev. B **86**, 115111 (2012).
[10] Y. Lu, M. Höppner, O. Gunnarsson, and M. W. Haverkort, Phys. Rev. B **90**, 085102 (2014).
[11] S.-K. Mo, J. D. Denlinger, H.-D. Kim, J.-H. Park, J. W. Allen, A. Sekiyama, A. Yamasaki, K. Kadono, S. Suga, Y. Saitoh, T. Muro, P. Metcalf, G. Keller, K. Held, V. Eyert, V. I. Anisimov, and D. Vollhardt, Phys. Rev. Lett. **90**, 186403 (2003).
[12] A. Sekiyama, H. Fujiwara, S. Imada, S. Suga, H. Eisaki, S. I. Uchida, K. Takegahara, H. Harima, Y. Saitoh, I. A. Nekrasov, G. Keller, D. E. Kondakov, A. V. Kozhevnikov, T. Pruschke, K. Held, D. Vollhardt, and V. I. Anisimov, Phys. Rev. Lett. **93**, 156402 (2004).
[13] H. Yokoyama, M. Ogata, and Y. Tanaka, J. Phys. Soc. Jpn. **75**, 114706 (2006); P. Phillips, Rev. Mod. Phys. **82**, 1719 (2010); T. Sato and H. Tsunetsugu, Phys. Rev. B **90**, 115114 (2014); S. Zhou, Y. Wang, and Z. Wang, Phys. Rev. B **89**, 195119 (2014); P. Prelovšek, J. Kokalj, Z. Lenarčič, and R. H. McKenzie, Phys. Rev. B **92**, 235155 (2015); S. Zhou, L. Liang, and Z. Wang, arXiv:1605.03597.
[14] K. G. Wilson, Rev. Mod. Phys. **47**, 773 (1975).
[15] R. Bulla, T. A. Costi, and T. Pruschke, Rev. Mod. Phys. **80**, 395 (2008).
[16] M. Bukov, M. Kolodrubetz, and A. Polkovnikov, Phys. Rev. Lett. **116**, 125301 (2016); M. Bukov, L. D'Alessio, and A. Polkovnikov, Adv. Phys. **64**, 139 (2015).
[17] S.-S. B. Lee, J. von Delft, and A. Weichselbaum, Phys. Rev. B **96**, 245106 (2017).
[18] S. Taie, R. Yamazaki, S. Sugawa, and Y. Takahashi, Nat. Phys. **8**, 825 (2012); C. Hofrichter, L. Riegger, F. Scazza, M. Höfer, D. R. Fernandes, I. Bloch, and S. Fölling, Phys. Rev. X **6**, 021030 (2016).
[19] A. Weichselbaum and J. von Delft, Phys. Rev. Lett. **99**, 076402 (2007); A. Weichselbaum, Phys. Rev. B **86**, 245124 (2012).
[20] A. Weichselbaum, Ann. Phys. (Amsterdam) **327**, 2972 (2012).
[21] See Supplemental Material at http://link.aps.org/supplemental/10.1103/PhysRevLett.119.236402, which contains Refs. [22–24], for additional numerical results and technical details.
[22] F. B. Anders and A. Schiller, Phys. Rev. Lett. **95**, 196801 (2005); Phys. Rev. B **74**, 245113 (2006).
[23] R. Bulla, A. C. Hewson, and T. Pruschke, J. Phys. Condens. Matter **10**, 8365 (1998).
[24] K. Byczuk, M. Kollar, K. Held, Y. F. Yang, I. A. Nekrasov, T. Pruschke, and D. Vollhardt, Nat. Phys. **3**, 168 (2007); C. Raas, P. Grete, and G. S. Uhrig, Phys. Rev. Lett. **102**, 076406 (2009).
[25] S.-S. B. Lee and A. Weichselbaum, Phys. Rev. B **94**, 235127 (2016).
[26] E. Müller-Hartmann, Z. Phys. B **76**, 211 (1989).
[27] R. Bulla, T. A. Costi, and D. Vollhardt, Phys. Rev. B **64**, 045103 (2001).
[28] C. Raas and G. S. Uhrig, Phys. Rev. B **79**, 115136 (2009).
[29] M. Hanl and A. Weichselbaum, Phys. Rev. B **89**, 075130 (2014).
[30] S. Nishimoto, F. Gebhard, and E. Jeckelmann, J. Phys. Condens. Matter **16**, 7063 (2004).
[31] E. Gull, D. R. Reichman, and A. J. Millis, Phys. Rev. B **82**, 075109 (2010).
[32] M. Granath and J. Schött, Phys. Rev. B **90**, 235129 (2014).
[33] A. B. Harris and R. V. Lange, Phys. Rev. **157**, 295 (1967); K. A. Chao, J. Spalek, and A. M. Oles, J. Phys. C **10**, L271 (1977); A. H. MacDonald, S. M. Girvin, and D. Yoshioka, Phys. Rev. B **37**, 9753 (1988); H. Eskes and A. M. Oleś, Phys. Rev. Lett. **73**, 1279 (1994); H. Eskes, A. M. Oleś, M. B. J. Meinders, and W. Stephan, Phys. Rev. B **50**, 17980 (1994); A. L. Chernyshev, D. Galanakis, P. Phillips, A. V. Rozhkov, and A.-M. S. Tremblay, Phys. Rev. B **70**, 235111 (2004).
[34] A. C. Hewson, *The Kondo Problem to Heavy Fermions* (Cambridge University Press, Cambridge, England, 1993).
[35] L. W. Cheuk, M. A. Nichols, K. R. Lawrence, M. Okan, H. Zhang, E. Khatami, N. Trivedi, T. Paiva, M. Rigol, and M. W. Zwierlein, Science **353**, 1260 (2016).